Microelectronic Engineering 124 (2014) 37–41

Contents lists available at ScienceDirect

Microelectronic Engineering

journal homepage: www.elsevier.com/locate/mee

Effect of bi-directional microfabricated topographical cues on cellular behavior of mammalian cell line

Y. Du [a], H.K. Woo [a], L. Li [a], K.Y. Mak [a], C.M. Wong [b,c], J. Shi [d], P.W.T. Pong [a,*]

[a] Department of Electrical and Electronic Engineering, The University of Hong Kong, Hong Kong
[b] Department of Pathology, The University of Hong Kong, Hong Kong
[c] State Key Laboratory for Liver Research, The University of Hong Kong, Hong Kong
[d] Department of Physics, Hong Kong Baptist University, Hong Kong

ARTICLE INFO

Article history:
Received 19 October 2013
Received in revised form 27 March 2014
Accepted 8 April 2014
Available online 18 April 2014

Keywords:
Mammalian cell line
Bi-directional stimuli
Contact guidance
Cell alignment

ABSTRACT

The study of cell migration is valuable for the understanding of various physiological and pathological processes. Microgrooved/microridged substrates have been intensively studied to reveal the effect of single topographical cues on cellular behavior. However, cells in vivo are usually surrounded by multidirectional topography signals. This study investigated the effect of bi-directional topographical cues on cellular behavior of mammalian cells. In this study, bi-directional pit patterned poly(dimethylsiloxane) (PDMS) substrates were fabricated with different sizes but same depth (1 μm). The fabricated patterns were then used to study cellular response to bi-directional cues of mammalian cell line, in this case HeLa cells. After seeding cells for 48 h, the PDMS substrates were examined by SEM. Cell alignment angle and aspect ratio were measured from the SEM images. The results show that the cells on the patterned substrates with square pits did not align along either *x*- or *y*-axis. However the patterns with rectangular pits could promote cell alignment along the longer sides of pits. Moreover, comparing to the cell elongation on the control flat substrate, the elongation of cells was decreased on all the patterned substrates. These results are helpful for a deeper understanding of the mechanism of bi-directional topographical cues on cellular behavior of mammalian cell line.

1. Introduction

Cells in human body are stimulated by the surrounded extracellular matrix (ECM) and they tend to migrate toward the more favorable orientation [1]. The study of cell migration is required for the understanding of various biological processes including embryonic development, tissue regeneration, and immune response [2]. In addition, the knowledge of cell migration is also important for tissue engineering in various medical applications including medical implants and pharmaceuticals [3]. The in vivo cell migration can be affected by various factors, such as chemoattractants, temperature, topography, and mechanical and tensile properties of ECM [3]. Among all these factors, the topographical property is spatially confined, visible, and stable. The pioneered work of Paul Weiss in 1958 reported the phenomena 'contact guidance' that cell migration responded to the underlying topography on micrometer and sub-micrometer scale [4,5]. Thus cell alignment can be guided by structures that mimic extracellular matrix (ECM) processes [6]. A recent study attributed contact guidance to cellular signaling processes [7]. Contact guidance is an essential regulator in cell migration for individual or groups of cells [8,9]. Consequently, the study of the effect of topographical cues on cell migration is critical for developing the fundamental knowledge of in vivo cell behavior.

Nowadays, different studies using artificial nano- or microstructured surfaces have been conducted to reveal the effect of topographical signals on cellular behavior. Among these structures, nano- or microgrooved/microridged surfaces are being used intensively for studies. They have been shown to exhibit great influences on cellular contact guidance of mammalian cells [10–12]. Studies of nanogratings reported that various cell types (endothelial progenitor cells (EPCs), bovine aortic endothelial cells (BAECs), human embryonic stem cells (HESCs), human mesenchymal stem cells (HMSCs), human embryonic kidney cells (HEK-293), and human foreskin fibroblasts) aligned and elongated in the direction of the grating axis [13–18]. The investigation of poly (dimethylsiloxane) (PDMS) substrates engraved with nano- and

* Corresponding author. Address: Room 607, Chow Yei Ching Building, Department of Electrical and Electronic Engineering, The University of Hong Kong, Pokfulam Road, Hong Kong. Tel.: +852 2857 8491.
E-mail address: ppong@eee.hku.hk (P.W.T. Pong).

http://dx.doi.org/10.1016/j.mee.2014.04.010
0167-9317/

microgrooves showed the alignment and elongation of BAECs along the groove directions [19]. Microgrooves on polystyrene substrates also have been reported to cause rat dermal fibroblasts (RDF) to align along the groove direction [20].

These previous studies were limited to stimulate cells along a single direction [3,21,22]. However, cells in vivo are subject to complex three-dimensional topographical features of ECM which cannot be fully represented by the single directional patterns [10]. It was recently found that bi-directional stimuli studies are important in understanding the fundamental mechanisms of how topography signals influence cellular behavior in vivo [21,22]. In this work, pit patterned PDMS substrates were fabricated and used to study cellular response of mammalian cell line, in this case HeLa cells. The size of each pit was smaller than a single cell. As a result, each cell could simultaneously experience topographical stimulation in two directions. This paper aimed to investigate the effect of bi-directional topographical cues on migration of HeLa cells.

2. Materials and methods for experiment

2.1. Fabrication of pit patterned PDMS substrates

In this study, PDMS substrates with pit patterns were fabricated by photolithography technology. The pits were separated by intersecting microridges and the patterns were defined by $R_X \times R_Y \times P_X \times P_Y$ as illustrated in Fig. 1(A). Seven types of pit pattern with the same depth (1 μm) were fabricated: $10 \times 10 \times 10 \times 10$, $5 \times 5 \times 5 \times 5$, $10 \times 10 \times 5 \times 5$, $5 \times 10 \times 5 \times 5$, $5 \times 5 \times 10 \times 5$, $5 \times 10 \times 10 \times 5$, and $5 \times 10 \times 5 \times 10$. All the units are micrometer (μm). In addition, a flat PDMS substrate was fabricated as control.

A simplified schematic diagram of the fabrication process is shown in Fig. 1(B). The pre-cleaned silicon wafers were spin coated with photoresist 5214E (AZ Electronic Materials). Then the photoresist was soft baked on a hotplate. In this study, photolithography was performed by SF-100 Xcel Platform (Intelligent Micro Patterning LL). The inverse patterns drawn by software AutoCAD (AutoDesk) were loaded into the system as image masks. After exposure and developing by AZ400K (AZ Electronic Materials), the inverse patterns were transferred to the photoresist layers. The resulting inverse patterned photoresist layers were then used as mask molds to fabricate the PDMS molds by casting. The PDMS molds, together with the master molds, were baked at 90 °C for 165 min. After cooling down, the PDMS molds were peeled off and used as the cell culturing substrates with pit patterns on the surface. One flat PDMS substrate was also fabricated by the same method using a pre-cleaned silicon wafer without photoresist.

2.2. Cell seeding

All the PDMS substrates were fixed into a 24-well cell culture cluster (Costar) and sterilized in 75% ethanol (EMSURE) for 1 h at room temperature. Afterwards, the ethanol was discarded and the substrates were rinsed with phosphate buffered saline (PBS, Gibco) to wash away residual ethanol. HeLa cells (American Type Culture Collection) at passage 16 were maintained in Dulbecco's Modified Eagle Medium (DMEM, Gibco) supplemented with 10% Fetal Bovine Serum (FBS, Gibco) and 1.1% Penicillin Streptomycin (Gibco), at 37 °C and 5% CO_2. In this experiment, HeLa cells were dissociated with 0.25% Trypsin–EDTA solution (Gibco) at room temperature for 5 min and seeded onto the PDMS substrates with a concentration of about 1×10^4 cells/cm^2. The cells were then incubated at 37 °C and 5% CO_2.

2.3. Cell fixing and imaging

Cells were cultured for about 48 h prior to fixing. After discharge the DMEM, the substrates were rinsed in PBS to remove all the unattached and dead cells. Then, the cells were fixed with 2.5% glutaraldehyde (GTA, Electron Microscopy Sciences) for 1 h and then washed three times with buffer Sodium Cacodylate Trihydrate (Electron Microscopy Sciences). Then, the cells were dehydrated by ethanol with gradually increasing concentration (25%, 50%, 70%, 90% and 100%, respectively), followed by critical-point drying (Bal-tec CPD030 critical point dryer). After sputtering with gold and gallium (Bal-Tec SCD005 sputter coating), the PDMS substrates with HeLa cells were examined by scanning electron microscope (SEM, Hitachi S-3400N Variable Pressure Scanning Electron Microscope). SEM images were evenly taken from various parts of each substrate and analyzed using software ImageJ (National Institute of Health). Cell alignment angle and aspect ratio were measured. Cell alignment angle was measured as the intersecting angle between the long axis of a cell and the *y* axis of the pattern. While on the control flat substrate, the *y* axis was defined by a randomly chosen straight line. Due to the symmetry of the alignment, all the angles larger than 90° were symmetrically folded to 0–90° range. The aspect ratio of a cell was defined by the major cell axis

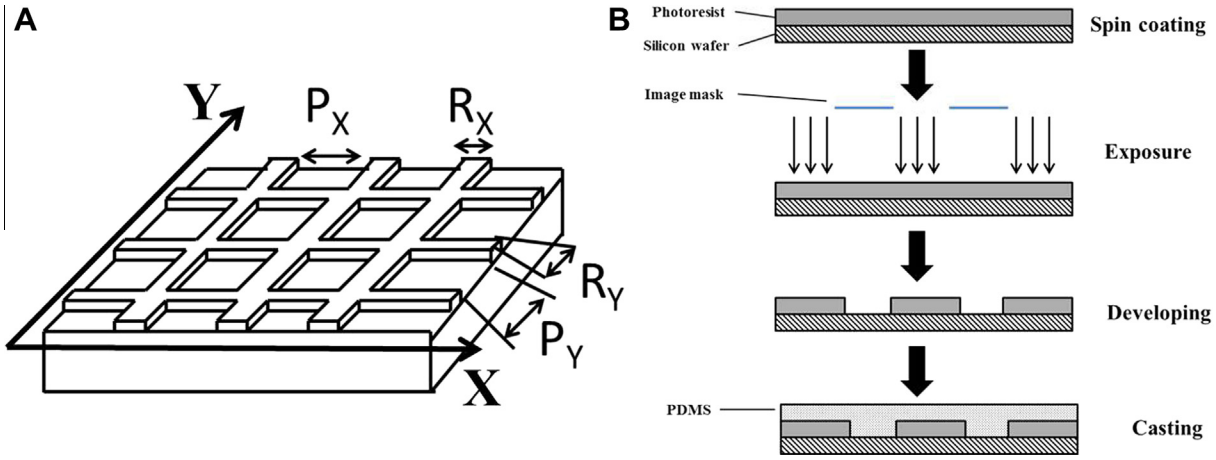

Fig. 1. Schematic diagrams of patterned PDMS substrates and fabrication process. (A) The pit patterned PDMS substrates were defined by $R_X \times R_Y \times P_X \times P_Y$ with R_X being the *x*-axis width of *y*-axis ridge, R_Y being the *y*-axis width of *x*-axis ridge, P_X being the *x*-axis width of pit, and P_Y being the *y*-axis width of pit. (B) Schematic diagram of the fabrication process of PDMS substrates. A pre-cleaned silicon wafer was spin coated with a uniform layer of photoresist. After exposure and developing, the inverse pattern from the image mask was transferred to the photoresist layer. Finally, PDMS substrate was fabricated by casting using the inverse patterned photoresist layer as the mask mold.

length divided by the minor cell axis length. Mean (M) and standard error of the mean (SE) were calculated for the aspect ratios, and the data are presented by M ± SE.

3. Results and discussion

In this study, HeLa cells were cultured on one control flat substrate and seven pit-patterned PDMS substrates for 48 h. The cellular alignment angle and aspect ratio were characterized based on SEM images. As shown in Fig. 2(A), the pit patterns were successfully produced on the PDMS substrate surfaces, and all SEM images were taken with the *x*-axis of the pattern in parallel to the bottom border of the image for convenience. While for the control flat substrate, as the cellular alignment angles were measured against a randomly chosen straight line, the SEM images were not oriented to any particular direction. SEM images were evenly taken from different parts of the PDMS substrates for analysis. The cells that linked or were in contact with neighboring cells were rejected for analysis. Examples are circled on Fig. 2(B). Single cells, as typically shown in Fig. 2(C) and (D), were used for analysis. There is no obvious difference between the morphology of cells cultured on the control flat substrate (Fig. 2(C)) and the patterned substrates (Fig. 2(D)). The cells shown in Fig. 2(C) and (D) both display an elongated and polygonal shape. The filopodia indicated by arrows radially extended. The highly dynamic filopodia were able to detect surrounding topography and served as topographical sensors [5]. As the pits were designed smaller than a single HeLa cell (Fig. 2(D)), each cell simultaneously covered more than one pit and experienced topographical stimulation in both *x* and *y* directions.

For the investigation of alignment angle, the angles between 90° and 180° described the same cellular orientations as their symmetrical angles about the *y*-axis. All the alignment angles between 90° and 180° were symmetrically folded to the 0–90° range. The results of the alignment angle measurement are shown in Fig. 3. Generally, the cell alignment angles were evenly distributed from 0° to 90° on the control flat substrate. It indicates that there was no obvious cell alignment to either *x*-axis or *y*-axis on the flat substrate. On the patterned substrates ($10 \times 10 \times 10 \times 10$, $5 \times 5 \times 5 \times 5$ and $10 \times 10 \times 5 \times 5$) with square pit (i.e. $P_X = P_Y$) and even X- and Y-ridge width (i.e. $R_X = R_Y$), the cell alignment angles were also evenly distributed from 0° to 90° as that on the flat substrate. Similar phenomena were observed on the patterned substrate ($5 \times 10 \times 5 \times 5$) with square pits (i.e. $P_X = P_Y$) but uneven X- and Y-ridge width (i.e. $R_X \neq R_Y$). Our results suggest that the cells on the pit-patterned substrates with square pits (i.e. $P_X = P_Y$) displayed random cell alignment, similar to that on the control flat substrate. The change of ridge width (R_X or R_Y) did not exert significant influence on cell alignment. For the two patterns having $P_X > P_Y$ ($5 \times 5 \times 10 \times 5$ and $5 \times 10 \times 10 \times 5$), the majority of cells (67% and 89% of cells, respectively) exhibited large alignment angles (from 45° to 90°), and there were no cells aligned close to the *y*-axis orientation (between 0° to 15° and 0° to 30°, respectively). It demonstrated that for these two patterns the cells tended to orient along the *x*-axis. On the contrary, for the pattern having $P_X < P_Y$ ($5 \times 10 \times 5 \times 10$), the majority of cells (83% of cells) exhibited small alignment angles (from 0° to 45°), and there were no cells aligned between 60° and 90°. This indicated the cells preferred to align along the *y*-axis on this pattern. In summary, only the patterns with rectangular pits (i.e. $P_X \neq P_Y$) could effectively promote cell alignment, and the HeLa cells tended to align along the direction of the longer side of the pits. This can be interpreted as the cells responded to the stronger contact guidance between the two directions which was provided by the longer side of the pits. In the previous research, grid micropatterns were fabricated to exert orthogonal stimulations to single cells (NIH3T3) [23,24]. It was reported that the longer side of the grid exerts stronger guiding effect to cells. Consequently, the cells were migrated specifically in the direction of the longer side of the rectangular grid. Our results agree with these previous studies.

Walboomers et al. reported a study about the contact guidance of RDF on microgrooved polystyrene substrates [20]. The grooves

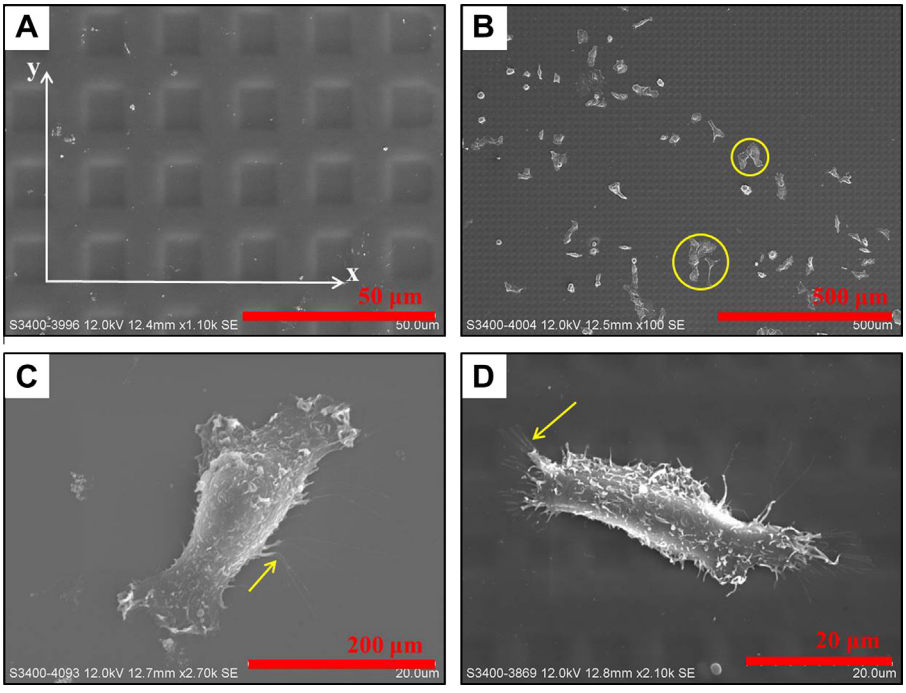

Fig. 2. SEM images of PDMS substrates. (A) SEM image of PDMS substrate with the $10 \times 10 \times 10 \times 10$ pattern transferred on it. (B) SEM image of $10 \times 10 \times 10 \times 10$ patterned PDMS substrate with HeLa cells on it. The circled cells are not suitable for analysis, because they linked or were in contact with neighboring cells. (C) SEM image of a single HeLa cell on the control flat substrate, and the arrow indicates the filopodia. (D) SEM image of a single HeLa cell on the $5 \times 10 \times 5 \times 5$ patterned substrate and the arrow indicates the filopodia.

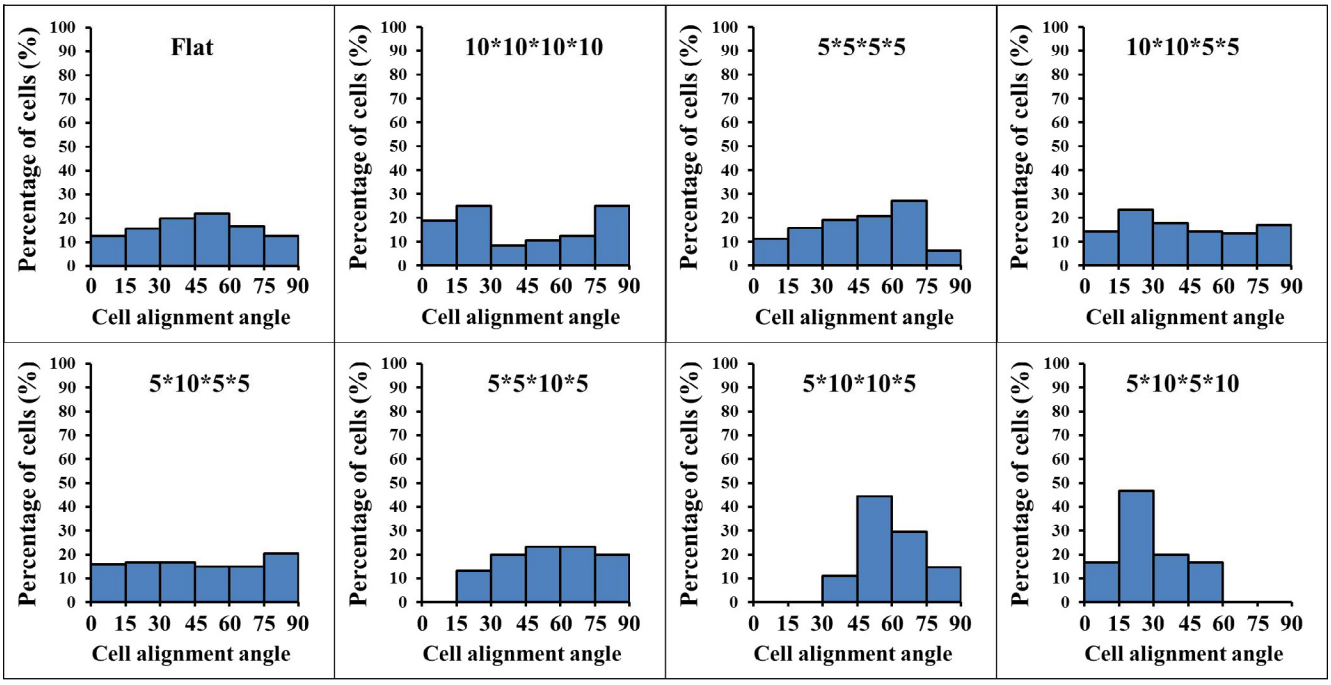

Fig. 3. Histograms of cell alignment angles for all eight patterns.

they fabricated had the same depth as our patterns (1 μm) and width between 1 and 10 μm. It was reported that the alignment angles for all the microgrooved patterns varied between 12.1° and 17.9°. Another study investigated the behavior of BAECs on microgroove patterned PDMS substrates [19]. The microgrooves with depth of 1 μm and width of 3.5 μm caused 90% of BAECs aligning within 20° against the grooves. Additionally, a study of HeLa cells cultured on microgrooved PDMS substrates with depth of 800 nm and width of 10 μm demonstrated that about 80% cells had alignment angle smaller than 10° against the microgrooves [25]. Apparently, the microgrooved patterns with depth of 1 μm or close to 1 μm (800 nm) caused significant contact guidance along the direction of the microgrooves, and the alignment angle were usually smaller than 20°. However, in our experiment, for the patterns with rectangular pits (i.e. $P_X \neq P_Y$), the average angles between the major axes of cells and the longer side of pits were around 34° ($5 \times 5 \times 10 \times 5$), 31° ($5 \times 10 \times 10 \times 5$) and 28° ($5 \times 10 \times 5 \times 10$), respectively. These results are larger than 20°. The cell alignment effect on the bi-directional patterned surfaces was weaker than that on the single directional microgrooved surfaces. The decrease of the alignment effect could be arisen from the competitive contact guidance from the orthogonal direction.

After 48 h culturing, the HeLa cells presented similar elongated shapes on the control flat and patterned substrates (Fig. 2(C) and (D)). The aspect ratios were calculated and results are shown in Fig. 4. Among all the results, the cellular aspect ratio of the control flat substrate was the largest (3.2 ± 0.1). The elongation of the HeLa cells decreased on the pit-patterned substrates. On the contrary, studies of single directional microgroove patterns reported that cell alignment was always coupled with stronger cell elongation along the edges of the grooves than on the flat surfaces [5]. This phenomena has been observed in various cell types, including epithelial cells, endothelial cells, smooth muscle cells, fibroblasts, stem cells, and Schwann cells [26]. However, studies about bi-directional patterns showed opposite conclusions. The cell spreading of HMSC on highly ordered nanopits were significantly reduced [27]. Decrease of cell spreading was also observed in the study of HeLa cell on nanopillar patterns [28]. These results agree with

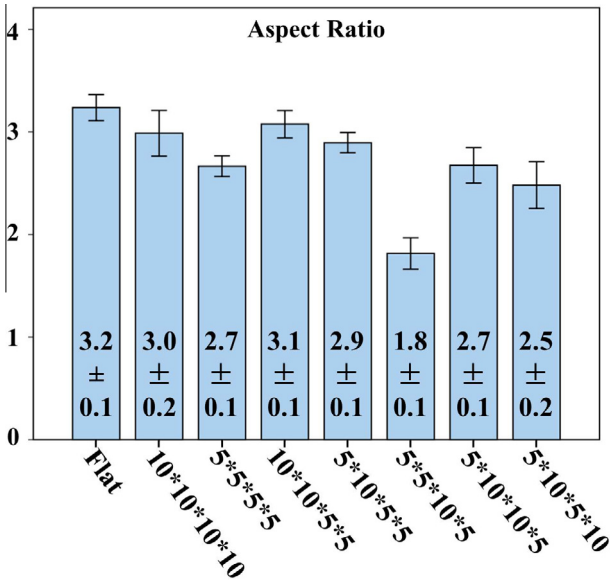

Fig. 4. Bar charts of experimental results for aspect ratio. The whiskers stand for the standard error of the mean (SE).

our results. The possible explanation for the differences between single directional and bi-directional patterns is that cells preferred to spread toward smooth surfaces, and dense patterns impeded the spread of cells. In this study, the elongation of the HeLa cells along the major axes was impeded by the pit patterns.

4. Conclusions

In this study, seven pit-patterned PDMS substrates were designed and fabricated to investigate the effect of bi-directional topographical cues on cellular behavior of HeLa cells. Independent of the change of ridge width, the cells on the patterned substrates with square pits (i.e. $P_X = P_Y$) displayed random cell alignment as

on the control flat substrates. On the other hand, the patterned substrates with rectangular pits (i.e. $P_X \neq P_Y$) could promote cell alignment along the longer sides of the pits. The contact guidance from the longer side of the pits was stronger than the shorter side, and the alignment of cells was the result of competition between the contact guidance at different directions. In addition, cell elongation was reduced on the pit-patterned substrates possibly because the pit edges impeded the spread of HeLa cells. Our finding suggests that both cell alignment and shape highly depended on the dimension of the bi-directional patterned structure. The HeLa cells responded to the patterns in a coordinated manner by comparing contact guidance from all directions. These provide physical insights on the fundamental mechanisms of bi-directional topographical influence on cellular behavior of mammalian cell line on micro-patterned surfaces which are useful for understanding of various biological processes and tissue engineering.

Acknowledgments

Y. Du and H.K. Woo contributed equally to this work. This work was supported by Seed Funding Program for Basic Research from the University of Hong Kong, Small Project Funding Program from the University of Hong Kong, ITF Tier 3 funding (ITS/112/12), RGC-GRF Grant (HKU 704911P), and University Grants Council of Hong Kong (Contract No. AoE/P-04/08).

References

[1] E. Martinez, E. Engel, J. Planell, J. Samitier, Ann. Anat. 191 (2009) 126–135.
[2] J. Mai, C. Sun, S. Li, X. Zhang, Biomed. Microdevices 9 (2007) 523–531.
[3] R. Flemming, C. Murphy, G. Abrams, S. Goodman, P. Nealey, Biomaterials 20 (1999) 573–588.
[4] P. Weiss, Int. Rev. Cytol. 7 (1958) 391–423.
[5] C.J. Bettinger, R. Langer, J.T. Borenstein, Angew. Chem. Int. Ed. 48 (2009) 5406–5415.
[6] D.A. Lauffenburger, A.F. Horwitz, Cell 84 (1996) 359–369.
[7] J.-R. Li, L. Shi, Z. Deng, S.H. Lo, G.-Y. Liu, Biochemistry 51 (2012) 5876–5893.
[8] K. Wolf, R. Müller, S. Borgmann, E.-B. Bröcker, P. Friedl, Blood 102 (2003) 3262–3269.
[9] P. Friedl, Curr. Opin. Cell Biol. 16 (2004) 14–23.
[10] X. Zhou, J. Hu, J. Li, J. Shi, Y. Chen, ACS Appl. Mater. Interfaces 4 (2012) 3888–3892.
[11] B.-Y. Yu, P.-H. Chou, Y.-M. Sun, Y.-T. Lee, T.-H. Young, J. Membr. Sci. 273 (2006) 31–37.
[12] X. Walboomers, J. Jansen, Biomaterials 21 (2000) 629–636.
[13] C.J. Bettinger, Z. Zhang, S. Gerecht, J.T. Borenstein, R. Langer, Adv. Mater. 20 (2008) 99–103.
[14] C.J. Bettinger, B. Orrick, A. Misra, R. Langer, J.T. Borenstein, Biomaterials 27 (2006) 2558–2565.
[15] S. Gerecht, C.J. Bettinger, Z. Zhang, J.T. Borenstein, G. Vunjak-Novakovic, R. Langer, Biomaterials 28 (2007) 4068–4077.
[16] E.K. Yim, S.W. Pang, K.W. Leong, Exp. Cell Res. 313 (2007) 1820–1829.
[17] E. Rebollar, I. Frischauf, M. Olbrich, T. Peterbauer, S. Hering, J. Preiner, P. Hinterdorfer, C. Romanin, J. Heitz, Biomaterials 29 (2008) 1796–1806.
[18] C.-H. Choi, S.H. Hagvall, B.M. Wu, J.C. Dunn, R.E. Beygui, Biomaterials 28 (2007) 1672–1679.
[19] P. Uttayarat, G.K. Toworfe, F. Dietrich, P.I. Lelkes, R.J. Composto, J. Biomed. Mater. Res., Part A 75 (2005) 668–680.
[20] X. Walboomers, H. Croes, L. Ginsel, J. Jansen, Biomaterials 19 (1998) 1861–1868.
[21] C.C. Berry, G. Campbell, A. Spadiccino, M. Robertson, A.S. Curtis, Biomaterials 25 (2004) 5781–5788.
[22] L. Moroni, L.P. Lee, J. Biomed. Mater. Res., Part A 88 (2009) 644–653.
[23] H. Jeon, H. Hidai, D.J. Hwang, K.E. Healy, C.P. Grigoropoulos, Biomaterials 31 (2010) 4286–4295.
[24] D.H. Kim, C.H. Seo, K. Han, K.W. Kwon, A. Levchenko, K.Y. Suh, Adv. Funct. Mater. 19 (2009) 1579–1586.
[25] X. Zhou, J. Shi, J. Hu, Y. Chen, Mater. Sci. Eng. C 33 (2012) 855–863.
[26] S.H. Hsu, C.Y. Chen, P.S. Lu, C.S. Lai, C.J. Chen, Biotechnol. Bioeng. 92 (2005) 579–588.
[27] A. Hart, N. Gadegaard, C.D. Wilkinson, R.O. Oreffo, M.J. Dalby, J. Mater. Sci. 18 (2007) 1211–1218.
[28] S. Nomura, Y. Ohyabu, K. Kuwabara, J. Artif. Organs 9 (2006) 90–96.